J. Cent. South Univ. (2022) 29: 1098−1106
DOI: https://doi.org/10.1007/s11771-022-4942-8

Springer

Impact of ultrasonic power on liquid fraction, microstructure and physical characteristics of A356 alloy molded through cooling slope

Pabak MOHAPATRA, Nirmal Kumar KUND

Department of Production Engineering, VSS University of Technology, Burla 768018, India

Abstract: This study involves A356 alloy molded through ultrasonically vibrated cooling slope. The slope alongside ultrasonic power enables indispensable shear for engendering slurry from which the semisolid cast/heat treated billets got produced. An examination demonstrates ultrasonically vibrated cooling slope influencing the liquid fraction/ microstructure/physical characteristics of stated billets. The investigation encompasses five diverse ultrasonic powers (0, 75, 150, 200, 250 W). The ultrasonic power of 150 W delivers finest/rounded microstructure with enhanced physical characteristics. Microstructural modifications reason physical transformations because of grain refinement and grain-boundary/Hall-Petch strengthening. A smaller grain size reasons a higher strength/shape factor and an increased homogeneity reasons a higher ductility. Microstructural characteristics get improved by reheating. It is owing to coalescence throughout temperature homogenization. The physical characteristics is improved by reheating because of a reduced porosity and enhanced dissolution besides augmented homogeneity. A direct comparison remains impossible owing to unavailability of researches on ultrasonically vibrated cooling slope.

Key words: ultrasonic power; microstructure; physical characteristics; semisolid cast; A356 alloy; cooling slope

Cite this article as: Pabak MOHAPATRA, Nirmal Kumar KUND. Impact of ultrasonic power on liquid fraction, microstructure and physical characteristics of A356 alloy molded through cooling slope [J]. Journal of Central South University, 2022, 29(4): 1098−1106. DOI: https://doi.org/10.1007/s11771-022-4942-8.

1 Introduction

Because of the strictly protective guidelines globally, mainly in transport segments, the focus further on manufacturing environmental materials with higher strength, less weight, more potential and greater safety is growing. On account of such necessities, the lightweighting is not an option but is the mandate. Besides, the use of biotechnology, natural fuels and battery operated automobiles creates an additional burden of weight. Certainly, the prospect has evolved since more than five decades for development of lighter materials with higher strength [1]. Since then aluminum alloys have been utilized widely for producing vehicle components [2]. The current study pertains to the technology of ultrasonic semisolid metal (USSM) processing [3−6].

The use of ultrasonic in material processing generates thixotropic microstructures of cast parts. Actually, there are three kinds of vibrations like mechanical, electromagnetic and ultrasonic [3]. Mechanical vibration involves unwarranted reaction between impeller and liquid metal because of direct contact between the impeller and liquid. Additionally, the use of high powered transducers makes ultrasonic technology superior than others [4,

Foundation item: Project(SAP-9162) supported by the Ministry of Mines, Technology Information, Forecasting and Assessment Council (TIFAC) and Department of Science and Technology (DST), India
Received date: 2020-12-10; **Accepted date:** 2021-05-13
Corresponding author: Nirmal Kumar KUND, PhD, Associate Professor; Tel: +91-9438865386; E-mail: nirmalkund@gmail. com; ORCID: https://orcid.org/0000-0002-3256-8288

5]. Effects of ultrasonic vibration of mould on microstructural properties were also illustrated in Ref. [6]. The investigations on the semisolid cast microstructures of AZ91 and A356 alloys through ultrasonic vibrations of mould were also demonstrated in Refs. [7, 8]. Microstructures of AZ31 and AZ61 alloys were produced through semisolid rolling and mechanically vibrating cooling slope [9, 10].

In addition, investigations on the use of cooling slopes were also reported in Refs. [11 − 14]. The influences of ultrasonic usage on solidification structure and mechanical behaviors of 6016 Al alloy were described in Ref. [15]. The effect of ultrasonic on microstructure and mechanical characteristics of slab casting was explained in Ref. [16]. Besides, ultrasonic green technology providing sustainability in melt processing was summarized in Ref. [17]. Equally, the microstructure growth in Al-Si alloy for ultrasonic casting processes was introduced in Ref. [18]. The influence of ultrasonic on mechanical properties of Al-Ni alloys was introduced in Ref. [19]. Additionally, the role of acoustic throughout sand mould casting of Al-Si alloy was elucidated in Ref. [20]. Furthermore, the influence of ultrasonic on segregation of secondary phase in Al-Cu alloy slab casting was revealed in Ref. [21]. The influence of cooling slope casting alongside heat treatment on microstructural/mechanical characteristics of A319-$x$$Mg_2Si$ composites was also investigated [22]. Dry sliding, structural and chemical behaviors of cast alloys/composites were also reported in Refs. [23−25].

Most of the related ultrasonic research reported is confined to mould vibrations throughout solidification (without use of cooling slope). Furthermore, few investigations on mechanically vibrated cooling slopes were also reported. With this perspective, the present research demonstrates experimental investigations on influences of ultrasonically vibrated cooling slope. Besides, physical characteristics of obtained products are evaluated with various material testing machines.

2 Experimental

Figure 1 demonstrates the experimental preparation of the ultrasonic system. It involves tundish and cooling slope. The cooling slope vibrates under diverse ultrasonic powers with an ultrasonic vibrator attached to the underneath of cooling slope. The molten alloy is dispensed inside mould cavity when passing the ultrasonically vibrated cooling slope. The ultrasonic power provides accelerated forced convection of the melt

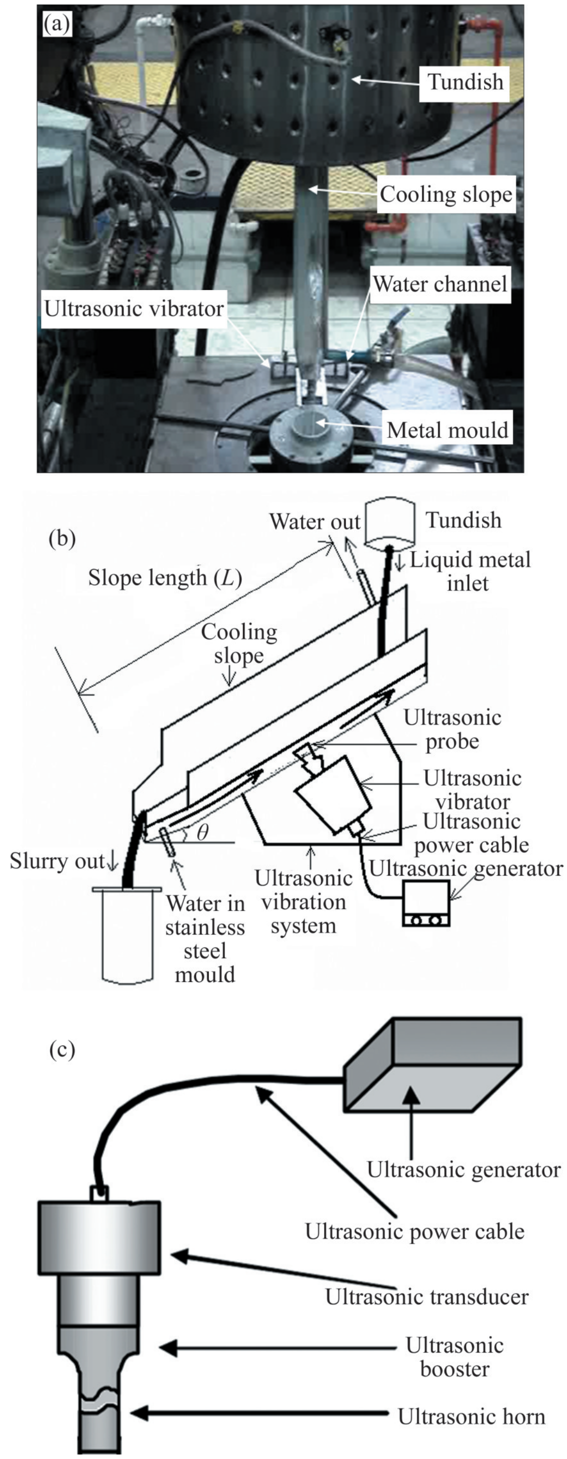

Figure 1 Details of experimental preparation: (a) Snapshot of experimental setup; (b) Schematic of experimental setup; (c) Schematic of ultrasonic system

with high powered transducers. In turn, it reasons enhanced homogeneity due to improved dendrite fragmentation and superior grain refinement. Besides, the most critical mechanism of ultrasonic power is the relationship between ultrasonic power and liquid phase rat. Therefore, experiments are conducted under ultrasonic powers of 0, 75, 150, 200 and 250 W with ultrasonic vibrator from underneath of the cooling slope.

2.1 Alloy melt production

A356 alloy nuggets are used in this study. A356 alloy melt is prepared in a SiC crucible, which was kept in an electric resistance furnace. The stated melt is treated with Al-Sr and Ti-B plaques for grain modification and refinement, respectively. The details about melt preparation and treatment have already been reported in Refs. [12, 13].

2.2 Alloy slurry preparation

1.5 kg of the liquid metal (at 625 °C) is slowly discharged inside mould cavity through ultrasonically vibrated cooling slope with length (L) of 250 mm and gradient (θ) of 60º. Using K-type thermocouple, the temperature of A356 alloy slurry is recorded at the slope exit. Here, the response time and measurement uncertainty of thermocouple are 0.8 s and $\pm 0.002T$ (T is in °C), respectively.

2.3 Billet production

Billets with size of 200 mm and radius of 20 mm are produced through solidification using the mentioned mould. To improve microstructures, several billets are heated using heating system, little beyond solidifying temperature. Additionally, the current induction reheating keeps semisolid cast billets at 580 ° C to produce the preferred heat treated billets.

2.4 Metallographic test sample production

Small pieces are carved from the obtained billets to get fragments with thickness of 10 mm. Diverse classes of emery sheets are utilized for finishing/refining disk-shaped specimens. Subsequently, finishing/refining for specimens of SiC powder and diamond paste is also completed. Consequently, finished/refined samples are etched with Keller's reagent [12, 13] at atmospheric conditions for metallographic analysis.

2.5 Microstructural characteristics

The microstructural characteristics like primary α-phase fraction, grain size, shape factor and particle density are evaluated for all cracked micrograph images of samples/specimens. Here, shape factor refers to globularity of particle represented by $4\pi S/C$, where S is the area and C is the perimeter. Its value varies between 0 (for dendrite) and 1 (for ideal circle). The details about microstructure morphology and characterization are not described here.

2.6 Physical characteristics

Tensile samples with gauge length of 20 mm and diameter of 4 mm are obtained from the produced billets. Tests about the stated samples are accomplished at ambient conditions using INSTRON 5567 with a strain rate of 0.001 s^{-1}. Furthermore, hardness test sections with diameter of 60 mm and thickness of 15 mm are produced from the billets. Hardness across concerned hardness test sections is measured with Zeiss UHL VMHT 0.001 Vickers hardness tester through diamond indenter with load of 1.96 N and dwell time of 20 s. For each case, around 5 samples and measurements are taken. Tensile and hardness tests are performed to examine strength, elongation and other physical characteristics of the A356 alloy billets.

3 Results and discussion

Experiments are conducted under five different ultrasonic powers (0, 75, 150, 200 and 250 W) to examin the influence of ultrasonically vibrated cooling slope on liquid fraction and billet characteristics. The higher ultrasonic power accelerates slurry flow over the cooling slope and hence, a small dwelling time for slurry over cooling slope is involved. Thus, slurry temperature at outlet of ultrasonically vibrated cooling slope increases with the ultrasonic power. Ultimately, liquid fraction increases with ultrasonic power. In other words, the increased ultrasonic power enhances melt flow and reduces residence/solidification time of plate over cooling slope. Hence, semisolid slurry temperature at slope exit increases with ultrasonic power. And solid fraction declines with the increase of ultrasonic power. Presently, the slurry temperatures at slope exit are 606, 608, 610, 612 and 614 °C for ultrasonic powers of 0, 75, 150, 200 and 250 W, respectively. Corresponding liquid fractions (which are determined by Scheil equation) are 75%, 79%, 83%, 87% and 91%, respectively. Figure 2 demonstrates the relationship between liquid fraction of slurry (accumulated in mould through ultrasonically vibrated cooling slope) and ultrasonic power.

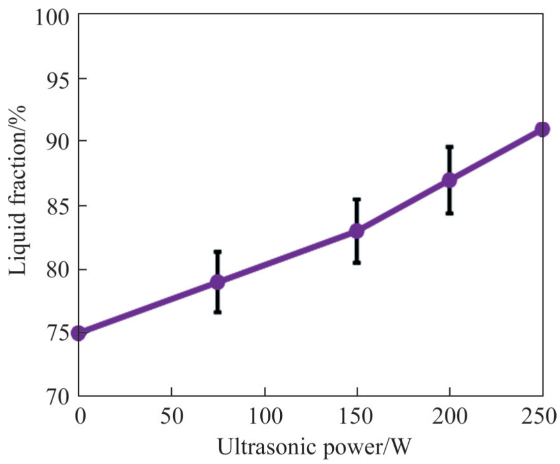

Figure 2 Liquid fraction vs ultrasonic power

3.1 Microstructure of cast billets

Five different semisolid cast billets are produced under five different ultrasonic powers. Specimens are prepared for quantitative or metallographic investigation. Figure 3 shows the microstructures of cast billets shaped under various ultrasonic powers.

Figure 4 demonstrates variations in microstructural characteristics of A356 alloy semisolid cast billets with ultrasonic power as observed after quantitative or metallographic investigation of micrographs. It can be witnessed that the grain size declines with rise in ultrasonic power up to 150 W. However, the grain density, primary α-phase fraction and shape factor rise with same up to stated limit. However, with further rise in ultrasonic power grain size rises, but grain density, primary α-phase fraction and shape factor decline. Eventually, the grain size, grain density, primary α-phase fraction and shape factor of the optimum globular microstructure materialized under 150 W ultrasonic power are 25 μm, 400, 0.92 and 0.88, respectively.

Instead, the ultrasonic vibration is also responsible for forced convections in melt. The forced convection can cause dendrite fragmentation

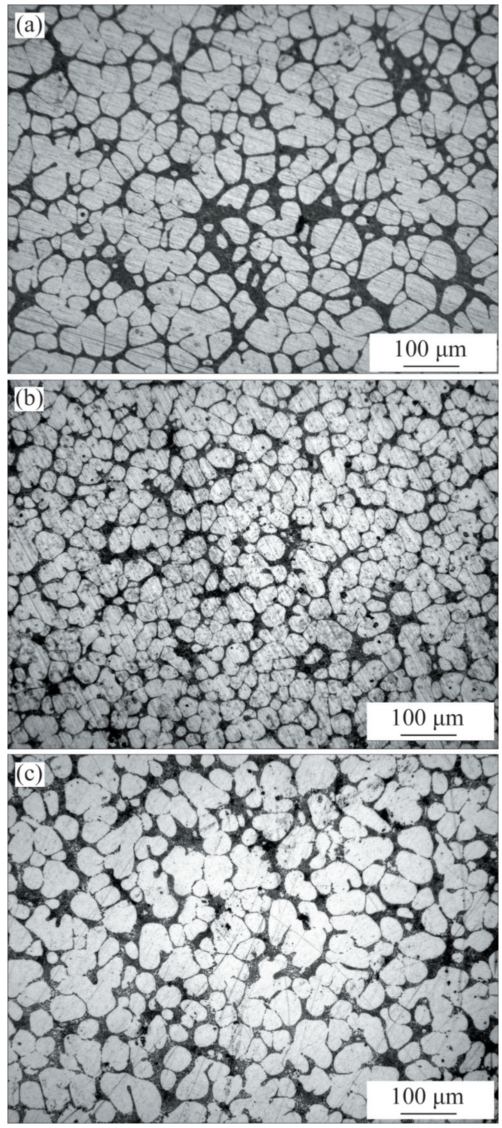

Figure 3 Microstructures of cast billets under different ultrasonic powers: (a) 0 W; (b) 150 W; (c) 250 W

and grain refinement, and thus increase the grain refinement until the ultrasonic power reaches 150 W. The forced convection can also cause coarsening owing to diffusion. And, coarsening (which decreases grain refinement) occurs when the ultrasonic power exceeds 150 W. Coarsening originates from coalescence/agglomeration with Ostwald ripening.

3.2 Microstructure of reheated billets

For enhancing surface texture, cast billets are heated until beyond solidifying temperature because eutectic phase melts during induction reheating, which increases flowability of the material. Furthermore, there is certain amount of melting at surface of α-phase during induction reheating,

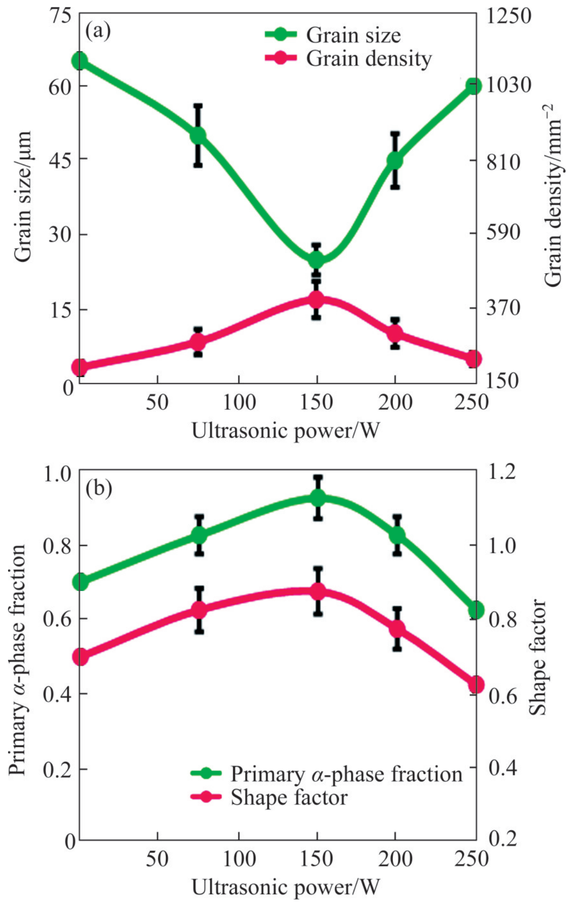

Figure 4 Microstructural characteristics of cast billets under different ultrasonic powers: (a) Grain size/grain density; (b) Primary α-phase fraction/shape factor

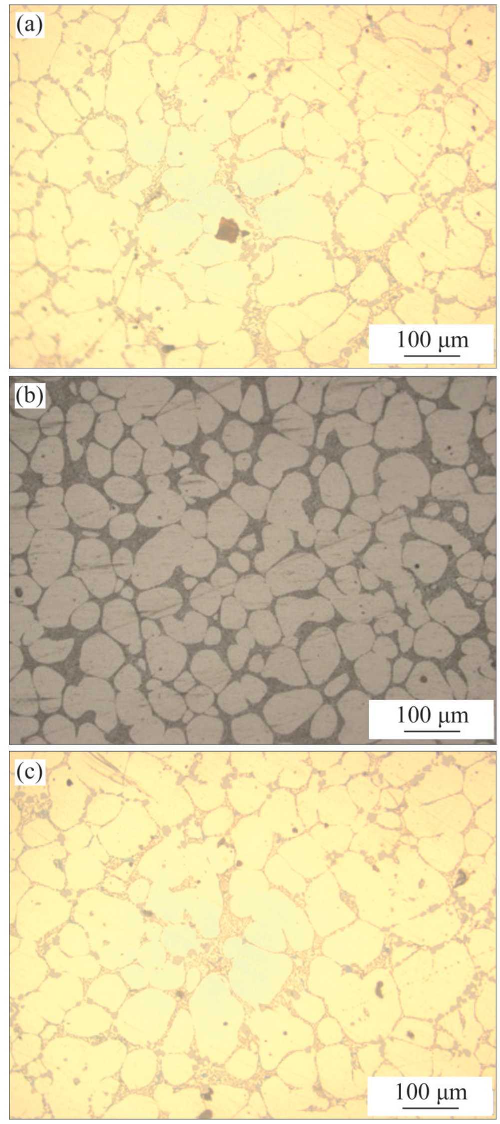

Figure 5 Microstructures of reheated billets under different ultrasonic powers: (a) 0 W; (b) 150 W; (c) 250 W

which transforms α-phase into globular structure. That is why specimens are got from reheated billets.

Figure 5 demonstrates typical microstructures of billets under different ultrasonic powers. Rounded microstructures are observed from all reheated billets. It is because temperature homogenization in billets throughout induction is repeated for around 10 min. However, the natures of variations with cooling slope by ultrasonic power remain the same. But, primary α-phase particles are comparatively larger.

Figure 6 demonstrates variations in microstructural characteristics of A356 alloy heat treated and semisolid cast billets under different ultrasonic powers. It is found that the natures of variations in microstructural characteristics with cooling slope by ultrasonic power are similar for both classes of billets. However, microstructural characteristics of heat treated billet is witnessed to be more or less even throughout domain. Additionally, the microstructural characteristics are improved when reheating. It is owing to coalescence throughout temperature homogenization. Liquid entrapping has also been observed.

With induction reheating, the grain size rises from 65, 25, 60 to 90, 50, 80 μm under ultrasonic power of 0, 150, 250 W, respectively (Figure 6(a)). Correspondingly, the grain density declines from 200, 400, 225 to 145, 250, 160 under ultrasonic power of 0, 150, 250 W, respectively. Additionally, primary α-phase fraction rises from 0.70, 0.92, 0.62 to 0.80, 0.95, 0.82 under ultrasonic power of 0, 150, 250 W, respectively (Figure 6(b)). In the meantime, shape factor rises from 0.7, 0.88, 0.62 to 0.8, 0.92, 0.72 under ultrasonic power of 0, 150, 250 W, respectively.

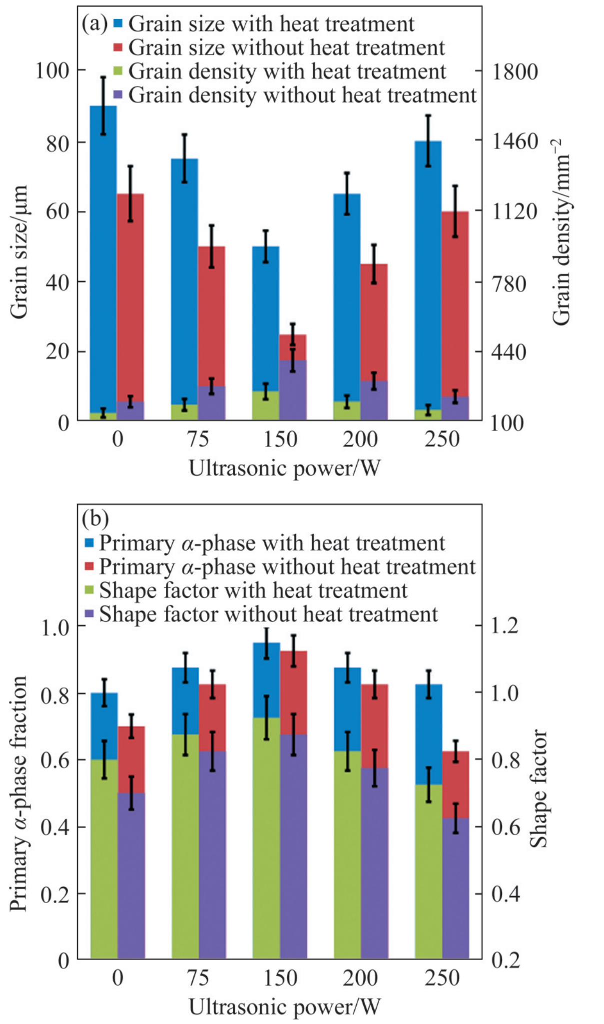

Figure 6 Variations in microstructural characteristics of cast and reheated billets with ultrasonic power: (a) Grain size/grain density; (b) Primary α-phase fraction/shape factor

It is observed that heat treatment absolutely influences ultimate microstructure and its microstructural characteristics. Instead, a straight comparison with outcomes of other reseachers is impossible because of unavailability of the stated type of researches (vis-a-vis ultrasonically vibrated cooling slope) in literature. The current examination provides enhanced microstructural characteristics as it encompasses their superior combination.

3.3 Physical characteristics of cast billets

Figure 7 demonstrates variations in physical characteristics (like tensile strength, elongation, yield strength and hardness) of A356 alloy semisolid cast billets under different ultrasonic powers. The stated physical characteristics rise with ultrasonic power until 150 W. However, with a further rise in ultrasonic power, the physical characteristics decline. The optimal physical characteristics are observed under ultrasonic power of 150 W and tensile strength, elongation, yield strength and hardness are 326 MPa, 17%, 254 MPa and HV 121, respectively.

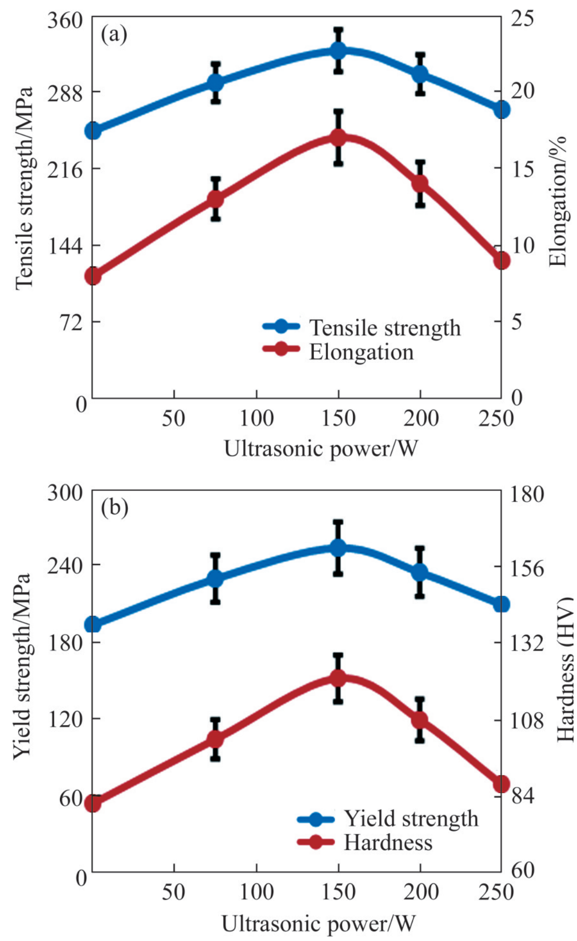

Figure 7 Physical characteristics of cast billets under different ultrasonic powers: (a) Tensile strength/elongation; (b) Yield strength/hardness

There may be two reasons for variations in the stated physical characteristics: 1) grain refinement along with homogeneity and 2) porosity. At large, the porosity makes strength, hardness decline besides ductility, which is the most important. However, the porosity has little influence (as compared with grain refinement) on physical characteristics of semisolid cast billets molded through ultrasonically vibrated cooling slope. Influence of grain refinement on physical characteristics may be fully realized from Hall-Petch effect. Indeed, smaller grain size reasons higher strength, while higher shape factor along with homogeneity reasons higher ductility.

3.4 Physical characteristics of heat treated billets

Figure 8 illustrates variations in physical characteristics of A356 alloy heat treated and semisolid cast billets under different ultrasonic powers. It is observed that variations in physical characteristics with cooling slope ultrasonic power remain quite identical for both classes of billets. However, physical characteristic of heat treated billet is observed to be more or less even throughout domain. The physical characteristics (like strength, hardness besides ductility) are enhanced with induction reheating. That is, reheated billets have better strength, hardness besides ductility compared with semisolid cast billets. It might be owing to less or quite negligible porosity and enhanced compositional elements dissolution in matrix besides improved chemical homogeneity. It is owing to particle coalescence throughout temperature homogenization.

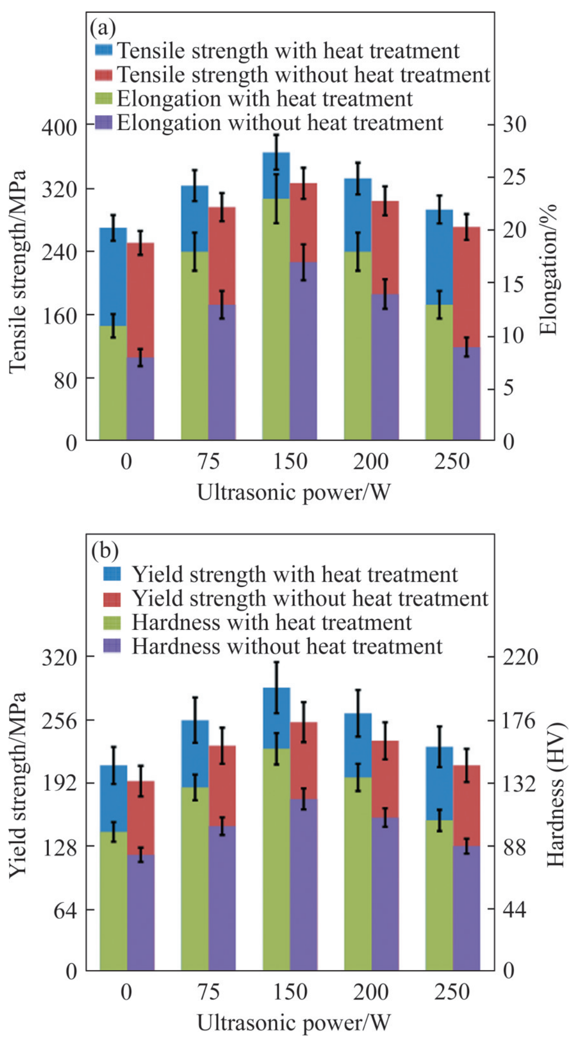

Figure 8 Physical characteristics of cast and reheated billets under different ultrasonic powers: (a) Tensile strength/elongation; (b) Yield strength/hardness

With induction reheating, the tensile performance rises from 251, 326, 271 to 270, 365, 293 MPa under ultrasonic power of 0, 150, 250 W, respectively (Figure 8(a)). Correspondingly, the elongation rises from 8%, 17%, 9% to 11%, 23%, 13% at ultrasonic power of 0, 150, 250 W, respectively. Additionally, the yield performance rises from 194, 254, 210 to 210, 289, 219 MPa under ultrasonic power of 0, 150, 250 W, respectively (Figure 8(b)). In the meatime, the hardness rises from HV 82, HV 121, HV 88 to HV 98, HV 156, HV 106 under ultrasonic power of 0, 150, 250 W, respectively.

It is witnessed that heat treatment certainly influences physical characteristics (like tensile strength, elongation, yield strength and hardness). Instead, a comparing directly using reported investigators' outcomes is impossible because of unavailability of stated type of investigations (i. e., ultrasonically vibrated cooling slope) in the text. It is also witnessed that the current examination delivers absolutely superior physical characteristics because it includes their optimal combination.

4 Conclusions

This study involved influence of ultrasonic power on solidification, microstructure and physical characteristics of A356 alloy molded through cooling slope (which is the first work of its kind). The grain size of semisolid cast/heat treated billets declined with an upsurge in cooling slope ultrasonic power up to 150 W. The grain density, primary α-phase fraction and shape factor have the same trend with grain size. However, with a further increasement in cooling slope ultrasonic power, the grain size augmented and grain density, primary α-phase fraction and shape factor declined. The ultimate and rounded microstructures (with the moderate microstructural characteristics) are observed under the ultrasonic power of 150 W applied on the cooling slope. Slight less ultrasonic power hindered dendrite fragmentation and grain refinement because of poor shearing with augmented grain size besides declined grain density, primary α-phase fraction and shape factor. Conversely, the slight more ultrasonic power triggered coarsening because of coalescence and

Ostwald ripening instigating the same. Furthermore, the physical characteristics (like strength, hardness and elongation) augmented with ultrasonic power up to 150 W thereafter declined with upsurge in ultrasonic power. Thus, the enhanced physical characteristics observed at ultrasonic power of 150 W applied on cooling slope. Stated variations in physical characteristics are witnessed primarily because of grain refinement associated with grain boundary strengthening or Hall-Petch strengthening. Thus, this indicated smaller grain size reasoning higher strength and higher shape factor along with homogeneity reasoning higher ductility. Additionally, the microstructural characteristics are improved by reheating. It is owing to coalescence throughout temperature homogenization. Liquid entrapping is also witnessed for some observations. Physical characteristics is also increased by induction reheating because of the reduced porosity, enhanced dissolution within matrix besides augmented chemical homogeneity. Natures of variations in microstructure and physical characteristics with ultrasonic power remain quite identical for both classes of billets. Instead, direct comparisons with outcomes of other investigators are impossible because of unavailability of stated type of researches (relation to ultrasonically vibrated cooling slope) in the literature. However, the present examination provides superior microstructural and physical characteristics as it encompasses their optimal combination.

Contributors

Nirmal Kumar KUND provided the concept and edited the draft of manuscript. Pabak MOHAPATRA conducted the literature review and wrote the first draft of the manuscript. Both authors replied to reviewers' comments and revised the final version.

Conflict of interest

Pabak MOHAPATRA and Nirmal Kumar KUND declare that they have no conflict of interest.

References

[1] FORM G W, WALLACE J F. Typical microstructure of cast metals [J]. Transactions of American Foundry Society, 1960, 68: 145−156.

[2] CAMPBELL J. Solidification technology in the foundry and casthouse [J]. The Metals Society, 1981, 273: 61−64.

[3] CAMPBELL J. Effects of vibration during solidification [J]. International Metals Reviews, 1981, 26(1): 71−108. DOI: 10.1179/imtr.1981.26.1.71.

[4] GAO De-ming, LI Zhi-jun, HAN Qing-you, et al. Effect of ultrasonic power on microstructure and mechanical properties of AZ91 alloy [J]. Materials Science and Engineering A, 2009, 502(1, 2): 2−5. DOI: 10.1016/j.msea.2008.12.005.

[5] ZHANG Zhi-qiang, LE Qi-chi, CUI Jian-zhong. Effect of high-intensity ultrasonic field on process of semi-continuous casting for AZ80 magnesium alloy billets [J]. Transactions of Nonferrous Metals Society of China, 2010, 20: s376−s381. DOI: 10.1016/S1003-6326(10)60501-8.

[6] YAO Lei, HAO Hai, JI Shou-hua, et al. Effects of ultrasonic vibration on solidification structure and properties of Mg-8Li-3Al alloy [J]. Transactions of Nonferrous Metals Society of China, 2011, 21(6): 1241−1246. DOI: 10.1016/S1003-6326(11)60848-0.

[7] ZHANG Liang, WU Guo-hua, WANG Shao-hua, et al. Effect of cooling condition on microstructure of semi-solid AZ91 slurry produced via ultrasonic vibration process [J]. Transactions of Nonferrous Metals Society of China, 2012, 22(10): 2357−2363. DOI: 10.1016/S1003-6326(11)61471-4.

[8] LÜ S, WU Shu-sen, DAI Wei, et al. The indirect ultrasonic vibration process for rheo-squeeze casting of A356 aluminum alloy [J]. Journal of Materials Processing Technology, 2012, 212(6): 1281−1287. DOI: 10.1016/j.jmatprotec.2012.01.018.

[9] GUAN Ren-guo, ZHAO Zhan-yong, WANG Xiang, et al. Process parameter optimizing and studies on microstructure and properties of AZ31 alloy prepared by semisolid rolling process [J]. Acta Metallurgica Sinica (English Letters), 2013, 26(3): 293−298. DOI: 10.1007/s40195-012-0190-5.

[10] ZHAO Zhan-yong, GUAN Ren-guo, WANG Xiang, et al. Microstructure formation mechanism and properties of AZ61 alloy processed by melt treatment with vibrating cooling slope and semisolid rolling [J]. Metals and Materials International, 2013, 19(5): 1063−1067. DOI: 10.1007/s12540-013-5022-2.

[11] KHOSRAVI H, AKHLAGHI F. Comparison of microstructure and wear resistance of A356-SiCp composites processed via compocasting and vibrating cooling slope [J]. Transactions of Nonferrous Metals Society of China, 2015, 25(8): 2490−2498. DOI: 10.1016/S1003-6326(15)63867-5.

[12] KUND N K, DUTTA P. Numerical study of solidification of A356 aluminum alloy flowing on an oblique plate with experimental validation [J]. Journal of the Taiwan Institute of Chemical Engineers, 2015, 51: 159−170. DOI: 10.1016/j.jtice.2015.01.002.

[13] KUND N K, DUTTA P. Numerical study of influence of oblique plate length and cooling rate on solidification and macrosegregation of A356 aluminum alloy melt with experimental comparison [J]. Journal of Alloys and Compounds, 2016, 678: 343−354. DOI: 10.1016/j.jallcom.2016.02.152.

[14] SAFFARI S, AKHLAGHI F. Microstructure and mechanical properties of Al-Mg_2Si composite fabricated in situ by vibrating cooling slope [J]. Transactions of Nonferrous

Metals Society of China, 2018, 28(4): 604－612. DOI: 10.1016/S1003-6326(18)64693-X.
[15] SHI Chen, SHEN Ke, MAO Da-heng, et al. Effects of ultrasonic treatment on microstructure and mechanical properties of 6016 aluminium alloy [J]. Materials Science and Technology, 2018, 34(12): 1511－1518. DOI: 10.1080/02670836.2018.1465514.
[16] SHI Chen, LI Fan, WU Yong-jun, et al. Effect of ultrasonic flexural vibration on solidification structure and mechanical properties of large-size 35CrMoV cast ingot [J]. Advances in Materials Science and Engineering, 2019, 2019: 1－8. DOI: 10.1155/2019/3421039.
[17] RIEDEL E, HORN I, STEIN N, et al. Ultrasonic treatment: A clean technology that supports sustainability in casting processes [J]. Procedia CIRP, 2019, 80: 101－107. DOI: 10.1016/j.procir.2019.01.110.
[18] CHANKITMUNKONG S, ESKIN D G, LIMMANEEVICHITR C. Microstructure evolution in an Al-Si piston alloy under ultrasonic melt processing [J]. IOP Conference Series: Materials Science and Engineering, 2019, 529(1): 012060. DOI: 10.1088/1757-899x/529/1/012060.
[19] SRIVASTAVA N, CHAUDHARI G P. Effect of ultrasonic treatment on the mechanical behaviour of Al-Ni alloys [J]. Materials Science and Technology, 2019, 35(10): 1239－1247. DOI: 10.1080/02670836.2019.1618621.
[20] PUGA H, BARBOSA J, CARNEIRO V H. The role of acoustic pressure during solidification of $AlSi_7Mg$ alloy in sand mold casting [J]. Metals, 2019, 9(5): 490. DOI: 10.3390/met9050490.
[21] PENG Hao, LI Rui-qing, LI Xiao-qian, et al. Effect of multi-source ultrasonic on segregation of Cu elements in large Al-Cu alloy cast ingot [J]. Materials (Basel, Switzerland), 2019, 12(17): E2828. DOI: 10.3390/ma12172828.
[22] YADAV D K, CHAKRABARTY I. Effect of cooling slope casting and partial remelting treatment on microstructure and mechanical properties of A319-$x$$Mg_2Si$ in-situ composites [J]. Materials Science and Engineering A, 2020, 791: 139790. DOI: 10.1016/j.msea.2020.139790.
[23] RADHIKA N, SAM M. Tribological and wear performance of centrifuge cast functional graded copper based composite at dry sliding conditions [J]. Journal of Central South University, 2019, 26(11): 2961−2973. DOI: 10.1007/s11771-019-4228-y.
[24] MA Jun, NIU Li-bin, YAN Yu-ting, et al. Influence of heat treatment on microstructure and electrochemical behaviors of Mg-Zn binary alloys prepared by gas-phase alloying technique [J]. Journal of Central South University, 2020, 27(3): 762−771. DOI: 10.1007/s11771-020-4329-7.
[25] CHU Chen-liang, WU Xiao-quan, QIU Shui-cai, et al. Microstructure and Gd-rich phase evolution of as-cast AZ31-xGd magnesium alloys during semi-solid isothermal heat treatment [J]. Journal of Central South University, 2021, 28(1): 1−15. DOI: 10.1007/s11771-020-4504-x.

(Edited by ZHENG Yu-tong)

中文导读

超声功率对冷却斜槽模压A356合金液相分数、微观组织及物理特性的影响

摘要：本文采用超声振动冷却斜槽对A356合金进行成型。超声振动冷却斜槽能剪切产生半固态铸造/热处理坯料的浆料，研究了5种不同的超声功率(0、75、150、200、250 W)下坯料的液相分数、显微组织、物理特性。当超声功率为150 W时，合金的微观组织更精细、圆整，物理特性更强。由于晶粒细化和晶界/Hall-Petch强化导致微观结构改变，从而导致物理性能改变。晶粒尺寸越小，强度/形状因子越高；晶粒均匀性越高，塑性越好。由于温度均匀化的合并作用，再加热改善了合金的微观组织；随着孔隙度的降低和溶解的增强以及均匀性的增强，在再加热过程中材料的物理性能得到改善。

关键词：超声波功率；微观结构；物理性能；半固体铸造；A356合金；冷却斜槽